

Point production of a nonrelativistic unparticle recoiling against a particle

Eric Braaten

*Department of Physics, The Ohio State University, Columbus, Ohio 43210, USA*Hans-Werner Hammer *Technische Universität Darmstadt, Department of Physics, Institut für Kernphysik,
64289 Darmstadt, Germany**and ExtreMe Matter Institute EMMI and Helmholtz Forschungsakademie Hessen für FAIR (HFHF),
GSI Helmholtzzentrum für Schwerionenforschung GmbH, 64291 Darmstadt, Germany*

(Received 16 January 2023; accepted 30 January 2023; published 21 February 2023)

A nonrelativistic unparticle can be defined as an excitation created by an operator with a definite scaling dimension in a nonrelativistic field theory with an approximate conformal symmetry. The point-production rate of an unparticle has power-law dependence on its total energy with an exponent determined by its scaling dimension. We use the exact result for the 3-point function of primary operators in a nonrelativistic conformal field theory to derive the contribution to the point production rate of the unparticle from its decay into another unparticle recoiling against a particle. In the case where the conformal symmetry is broken by a large positive scattering length, we deduce the exponent of the energy in the point production rate of the loosely bound two-particle state recoiling against a particle with large relative momentum.

DOI: [10.1103/PhysRevD.107.034017](https://doi.org/10.1103/PhysRevD.107.034017)

I. INTRODUCTION

A definition of an *elementary particle* that is popular in group-theoretic circles is an irreducible representation of the Poincaré group. The concept of an *unparticle* was introduced by Georgi [1]. An unparticle is a system created by a local operator with a definite scaling dimension in a conformal field theory (CFT). It can therefore be defined as an irreducible representation of the conformal symmetry group. The conformal group on a $(3 + 1)$ -dimensional Minkowski space-time is a 15-dimensional group that includes the Poincaré group and scale transformations as subgroups. A relativistic unparticle is characterized by a single number: the scaling dimension of the operator. If the CFT belongs to a hidden sector beyond the Standard Model of particle physics, the unparticle cannot be observed directly. However it can be observed indirectly through the momentum distribution of Standard Model particles produced in association with the unparticle [1]. If the unparticle is produced in association with a single Standard Model particle, the invariant mass distribution of the unparticle can be determined by measuring the recoil-momentum distribution of the Standard Model particle.

It has power-law behavior with an exponent determined by the scaling dimension of the unparticle. The existence of unparticles in a hidden sector would produce novel signals in high energy colliders [2–4]. The CMS Collaboration has searched for signals of unparticles in pp collisions at the Large Hadron Collider [5–7].

Hammer and Son recently pointed out that unparticles can also arise in nonrelativistic physics [8]. The nonrelativistic conformal symmetry group on a $(3 + 1)$ -dimensional Galilean space-time is a 13-dimensional group that includes the Galilean group and scale transformations as subgroups.¹ It is also called the Schrödinger group, because it is the symmetry group of the free Schrödinger equation. A nonrelativistic conformal field theory (NRCFT) is a field theory with nonrelativistic conformal symmetry [10]. A *nonrelativistic unparticle* is a system created by a local operator with a definite scaling dimension in such a theory. In contrast to the relativistic case, a nonrelativistic unparticle is characterized by two numbers: its kinetic mass M and the scaling dimension Δ of the operator [8].

Hammer and Son pointed out that systems of low-energy neutrons produced by a short-distance reaction provide physical examples of nonrelativistic unparticles [8]. Neutrons have a negative scattering length a that is much larger than their effective range r_0 . As a consequence, the behavior of a system of neutrons whose kinetic energies in

Published by the American Physical Society under the terms of the Creative Commons Attribution 4.0 International license. Further distribution of this work must maintain attribution to the author(s) and the published article's title, journal citation, and DOI. Funded by SCOAP³.

¹For a discussion of the relation to the relativistic conformal group, see e.g. Ref. [9].

their center-of-momentum (CM) frame are all in the scaling region between $1/(m_n a^2)$ and $1/(m_n r_0^2)$, where m_n is the neutron mass, is approximately scale invariant. In the unitary limit $1/a \rightarrow 0$, $r_0 \rightarrow 0$, a nonrelativistic effective field theory describing the neutrons has nonrelativistic conformal symmetry. A convenient basis for local operators in the effective field theory are those with definite scaling behavior under the conformal symmetry. A system of N neutrons created by a local operator with scaling dimension Δ_N can be interpreted as an unparticle with mass Nm_n . For the 2-neutron unparticle, the lowest scaling dimension is $\Delta_2 = 2$. For unparticles with larger N , the scaling dimensions are transcendental numbers. For the 3-neutron unparticle, the lowest scaling dimension is $\Delta_3 = 4.27272$. The lowest scaling dimensions for 4 and 5 neutrons are 5.07 and 7.6, respectively. A summary of the lowest scaling dimensions for up to six neutrons is given in Table I of [10].

An N -neutron unparticle can be created by a short-distance nuclear reaction of the form $A_1 + A_2 \rightarrow B + (nn\dots)$ [8]. The invariant energy E of the N neutrons, which is their total kinetic energy in their CM frame, can be determined by measuring the momentum of the recoiling nucleus B or by detecting the neutrons directly. There is a scaling region of E in which the differential cross section has the scaling behavior $E^{\Delta_N - 5/2} dE$. The corresponding power-law behavior for N noninteracting particles as E approaches the threshold is governed by the N -particle phase space, $E^{(3N-5)/2} dE$. In the case of fermions, there is an additional Pauli suppression factor E for each pair of identical particles. For E of the order of the energy scale set by the neutron-neutron scattering length $\epsilon_{nn} = 1/(m_n a^2)$, there is a transition from the phase-space behavior for noninteracting particles to the power-law behavior governed by Δ_N in the scaling region. This nontrivial scaling behavior is the smoking gun for an unparticle. The resulting predictions for the invariant energy distributions of 2, 3, and 4 neutrons are shown in Fig. 1. In the case of 2 neutrons, there is a maximum in the region $E \sim \epsilon_{nn}$. For larger neutron numbers, there is a change in the slope of the log-log plot in the region $E \sim \epsilon_{nn}$.

The predicted invariant energy distribution, dR/dE , for four neutrons in Fig. 1 is not consistent with a resonance-like structure at $E/\epsilon_{nn} \approx 20$ in the point production of four neutrons. Such a structure was recently observed in the $4n$ spectrum measured in the knock-out reaction ${}^8\text{He}(p, p\alpha)4n$ by Duer *et al.* [11]. However, the neutron distribution of the initial ${}^8\text{He}$ nucleus clearly plays a role in this process and the applicability of the point-production approximation is questionable as the neutrons are emitted from a ${}^8\text{He}$ source. A recent theoretical study of the reaction [12] attributes the structure to the final-state interaction among the four neutrons and the presence of preexisting four neutrons in the periphery of the ${}^8\text{He}$ nucleus projectile. While the former effect is captured in the invariant $4n$ energy distribution of Fig. 1, the latter is not.

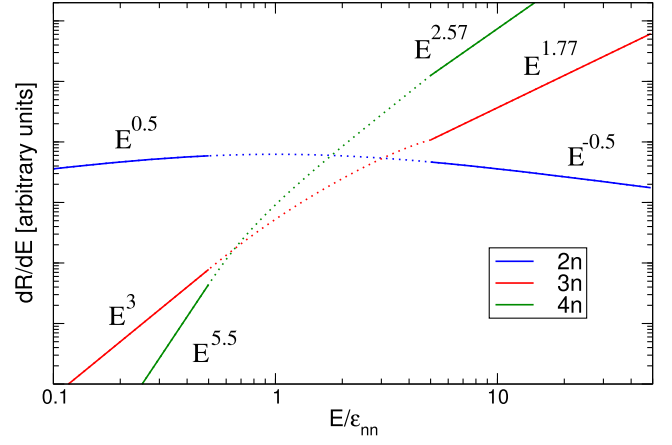


FIG. 1. Scaling prediction of Ref. [8] for the invariant energy distribution dR/dE of 2, 3, and 4 neutrons in their CM frame. The transition from the free phase-space behavior to the scaling region around $E \sim \epsilon_{nn}$ is illustrated by the dotted lines.

In Ref. [13], we pointed out that a low-energy system of neutral charm mesons created by a short-distance reaction is an unparticle because of the $X(3872)$ resonance in the $D^{*0}\bar{D}^0 + D^0\bar{D}^{*0}$ channel [14]. The scattering length a in that channel is large and negative. Because the resonant channel is a superposition of charm mesons, there is no Efimov effect [15,16]. The behavior of a system of neutral charm mesons whose kinetic energies in their CM frame are all in the scaling region between $1/(2\mu a^2)$ and $1/(2\mu r_0^2)$, where μ is the reduced mass of D^{*0} and \bar{D}^0 , is therefore approximately scale invariant. In the unitary limit $1/a \rightarrow 0$, $r_0 \rightarrow 0$, a nonrelativistic effective field theory describing the neutral charm mesons has nonrelativistic conformal symmetry. A convenient basis for local operators in the effective field theory are those with definite scaling behavior under the conformal symmetry. A system of N neutral charm mesons created by a local operator with scaling dimension Δ_N can be interpreted as an unparticle. The scaling dimensions for 2-charm-meson unparticles are the same as for two neutrons. The lowest scaling dimensions for 3-charm-meson unparticles are $\Delta_3 = 3.10119$ for $D^0\bar{D}^{*0}D^0$ and $\bar{D}^0D^{*0}\bar{D}^0$ as well as $\Delta_3 = 3.08697$ for $D^0\bar{D}^{*0}\bar{D}^{*0}$ and $\bar{D}^0D^{*0}D^{*0}$. In each case, there are two pairs of particles with a large scattering length a . The slight difference in the two values of Δ_3 is due to the different masses of the D^0 and D^{*0} . The 2-charm-meson unparticle can be observed through the recoil-momentum spectrum of the kaon in the inclusive decay $B^\pm \rightarrow K^\pm + (\text{anything})$. A 3-charm-meson unparticle can be observed through the prompt production of $X(3872)D^0$ at the Large Hadron Collider.

Because the scattering length a in the case of neutral charm mesons is large and positive, the unparticles have components that include bound states. There are reactions for producing final states that include bound states whose

rates have power-law behavior with exponents determined by conformal symmetry. The simplest such reaction is the production of $X(3872)D^0$ from the creation of a 3-charm-meson unparticle at a point, whose rate scales as a power of the unparticle energy E [13].

In this paper, we consider the production of a pair of unparticles from the creation of a single unparticle at a point. We use the analytic result for the 3-point function of primary operators in a NRCFT to derive the contribution to the production rate from another unparticle recoiling against a single particle. In the case where the conformal symmetry is broken by a large positive scattering length, we deduce the exponent of the energy in the point production rate of the loosely bound two-particle state recoiling against a particle with large relative momentum.

II. THREE-POINT FUNCTION FOR PRIMARY OPERATORS

We start by calculating the Fourier transform of the 3-point function for primary operators in a NRCFT. We take the dimension of space to be D , and we denote a space-time position by $x = (\mathbf{x}, t)$. An operator $\phi_3^\dagger(x)$ with scaling dimension Δ_3 creates an unparticle with mass M_3 . An operator $\phi_2(x)$ with scaling dimension Δ_2 annihilates an unparticle with mass M_2 . An operator $\phi_1(x)$ with scaling dimension Δ_1 annihilates an unparticle with mass $M_1 = M$. The masses satisfy the constraint $M_1 + M_2 = M_3$ from Galilean symmetry. We are particularly interested in the case where $\phi_1(x)$ annihilates a single particle with mass M , in which case its scaling dimension is $\Delta_1 = D/2$.

A. Propagators

The space-time propagator for a primary operator $\phi_n(x)$ with mass M_n and scaling dimension Δ_n is

$$\langle \phi_n(x_1) \phi_n^\dagger(x_2) \rangle = C_n (t_{12})^{-\Delta_n} \theta(t_{12}) \exp\left(i \frac{M_n x_{12}^2}{2t_{12}}\right), \quad (1)$$

where $t_{ij} = t_i - t_j$, $x_{ij}^2 = (\mathbf{x}_i - \mathbf{x}_j)^2$, and C_n is a constant. We represent the space-time propagator by the diagram in Fig. 2.

The energy-momentum propagator is obtained by Fourier transforming in both space-time positions and then factoring out an energy-momentum delta function. It is advantageous to take the variables $(x_1 + x_2)/2$ and $x_1 - x_2$ for the Fourier transform. After performing the trivial

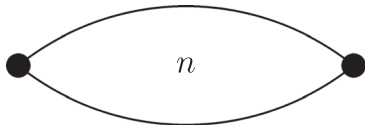


FIG. 2. Space-time propagator for unparticle n with kinetic mass M_n and scaling dimension Δ_n .

Fourier transform in $(x_1 + x_2)/2$, the remaining Fourier transform in space is a Gaussian integral that depends on the momentum \mathbf{p} ,

$$\begin{aligned} & \int d^D x_{12} \exp\left(-i\mathbf{p} \cdot \mathbf{x}_{12} + i \frac{M_n x_{12}^2}{2t_{12}}\right) \\ &= \left(2\pi i \frac{t_{12}}{M_n}\right)^{D/2} \exp\left(-i \frac{t_{12}}{2M_n} p^2\right). \end{aligned} \quad (2)$$

The subsequent Fourier transform in time gives a simple function of the energy E ,

$$\begin{aligned} & \int_0^\infty dt_{12} (it_{12})^{D/2 - \Delta_n} \exp\left(iEt_{12} - i \frac{p^2}{2M_n} t_{12}\right) \\ &= -i\Gamma\left(\frac{D}{2} + 1 - \Delta_n\right) \left(\frac{p^2}{2M_n} - E\right)^{\Delta_n - D/2 - 1}. \end{aligned} \quad (3)$$

With an appropriate choice for the constant C_n in Eq. (1), our final result for the energy-momentum propagator is

$$D_n(E, p) = -iC'_n \left(\frac{p^2}{2M_n} - E\right)^{\Delta_n - D/2 - 1}, \quad (4)$$

where C'_n is a constant.

In the case where $\phi_1(x)$ annihilates a single particle, its scaling dimension is $\Delta_1 = D/2$ and the propagator in Eq. (4) has a simple pole in the energy E at $p^2/(2M)$. With the conventional choice $C'_1 = 1$, the discontinuity in the energy is

$$D_1(E + i\epsilon, p) - D_1(E - i\epsilon, p) = 2\pi\delta\left(E - \frac{p^2}{2M}\right). \quad (5)$$

For other unparticles, the discontinuity in the energy is

$$\begin{aligned} & D_n(E + i\epsilon, p) - D_n(E - i\epsilon, p) \\ &= 2C'_n \sin(\pi(\Delta_n - D/2)) \left(E - \frac{p^2}{2M_n}\right)^{\Delta_n - D/2 - 1} \\ &\quad \times \theta\left(E - \frac{p^2}{2M_n}\right). \end{aligned} \quad (6)$$

B. Space-time three-point function

The 3-point function $\langle \phi_1(x_1) \phi_2(x_2) \phi_3^\dagger(x_3) \rangle$ for primary operators in a NRCFT was first considered by Henkel in 1993 [17]. The 3-point function can be represented by the diagram in Fig. 3. He used the Schrödinger symmetry to determine the 3-point function analytically up to a scaling function of a single variable,

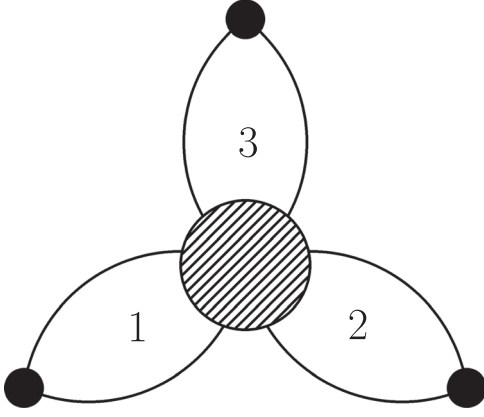


FIG. 3. Space-time 3-point function for primary operators associated with unparticles 1, 2, and 3.

$$\begin{aligned} \langle \phi_1(x_1) \phi_2(x_2) \phi_3^\dagger(x_3) \rangle &= (t_{13})^{-\Delta_{13,2}/2} \theta(t_{13}) \exp\left(i \frac{M_1 x_{13}^2}{2t_{13}}\right) \\ &\times (t_{23})^{-\Delta_{23,1}/2} \theta(t_{23}) \exp\left(i \frac{M_2 x_{23}^2}{2t_{23}}\right) \\ &\times (t_{12})^{-\Delta_{12,3}/2} \Phi(w), \end{aligned} \quad (7)$$

where $\Delta_{ij,k} = \Delta_i + \Delta_j - \Delta_k$ and the argument of the scaling function Φ is

$$w = \frac{(t_{23}(\mathbf{x}_1 - \mathbf{x}_3) - t_{13}(\mathbf{x}_2 - \mathbf{x}_3))^2}{2t_{13}t_{23}t_{12}} = \frac{1}{2} \left(\frac{x_{12}^2}{t_{12}} - \frac{x_{13}^2}{t_{13}} + \frac{x_{23}^2}{t_{23}} \right). \quad (8)$$

The first expression shows that the sign of w is the same as the sign of t_{12} . The scaling function $\Phi(w)$ depends also on the masses M_1 and M_2 and on the scaling dimensions Δ_1 , Δ_2 , and Δ_3 . The 3-point function in Eq. (7) is symmetric under the interchange of the subscripts 1 and 2.

An integral representation for the scaling function $\Phi(w)$ was first obtained by Henkel and Unterberger from the 3-point function for a CFT in two higher dimensions [18]. It has also been obtained by Fuertes and Moroz and by Volovich and Wen using holography and the AdS/CFT correspondence [19,20]. In the anti-de Sitter space (AdS) formulation, the external points in Fig. 3 are on the boundary of AdS and the blob is replaced by a point interaction inside the bulk of AdS. In Refs. [18,19], the 3-point function is expressed as a function of Euclidean

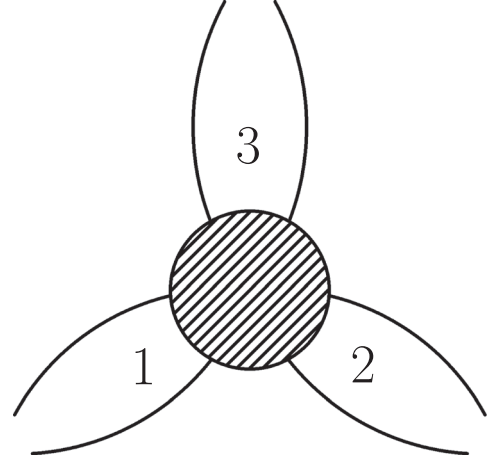


FIG. 4. Fourier-transformed 3-point function for primary operators associated with unparticles 1, 2, and 3.

times. The expression in Ref. [20] in terms of real times is more directly useful for our purposes. The integral representation for the scaling function is

$$\begin{aligned} \Phi(w) &= C_{12,3} \int_{-\infty}^{+\infty} du (u + i\epsilon)^{-\Delta_{13,2}/2} e^{-iM_1 u} \\ &\times \int_{-\infty}^{+\infty} dv (v + i\epsilon)^{-\Delta_{23,1}/2} e^{-iM_2 v} \\ &\times [u - v + (1 + i\epsilon)w]^{-\Delta_{12,3}/2}, \end{aligned} \quad (9)$$

where $C_{12,3}$ is a constant. Because the signs of t_{12} and w are identical [cf. Eq. (8)], the product of $(t_{12})^{-\Delta_{12,3}/2}$ and the last factor in Eq. (9) has a well-defined imaginary part,

$$\begin{aligned} (t_{12})^{-\Delta_{12,3}/2} [u - v + (1 + i\epsilon)w]^{-\Delta_{12,3}/2} \\ = [t_{12}(u - v + w) + i\epsilon]^{-\Delta_{12,3}/2}. \end{aligned} \quad (10)$$

The scaling function can also be expressed analytically in terms of a confluent hypergeometric function [20].

C. Fourier transform in space

The Fourier transform of the 3-point function in position space can be represented by the diagram in Fig. 4. To evaluate the Fourier transforms in the three spatial positions, it is convenient to express the last factor in Eq. (10) as the integral of an exponential,

$$[t_{12}(u - v + w) + i\epsilon]^{-\Delta_{12,3}/2} = (e^{i\pi/2} |t_{12}|)^{-\Delta_{12,3}/2} \frac{1}{\Gamma(\Delta_{12,3}/2)} \int_0^\infty dm m^{\Delta_{12,3}/2-1} \exp(-m[\epsilon - i\text{sign}(t_{12})(u - v + w)]). \quad (11)$$

The Fourier transform can be expressed as the product of the momentum-conserving delta function $\delta^D(\mathbf{p}_1 + \mathbf{p}_2 - \mathbf{p}_3)$ and a Gaussian integral in \mathbf{x}_{13} and \mathbf{x}_{23} . In the case $t_{12} > 0$, the Gaussian integral is

$$\begin{aligned}
& \int d^D x_{13} \exp\left(-i\mathbf{p}_1 \cdot \mathbf{x}_{13} + i\frac{M_1 x_{13}^2}{2t_{13}}\right) \int d^D x_{23} \exp\left(-i\mathbf{p}_2 \cdot \mathbf{x}_{23} + i\frac{M_2 x_{23}^2}{2t_{23}}\right) e^{+imw} \\
&= \left(2\pi i \frac{t_{12} t_{13}}{t_{12} M_1 + t_{23} m}\right)^{D/2} \left(2\pi i \frac{t_{23}(t_{12} M_1 + t_{23} m)}{t_{12} M_1 M_2 + t_{13} M_1 m + t_{23} M_2 m}\right)^{D/2} \\
&\quad \times \exp\left(-i \frac{t_{12} t_{13} (M_2 + m) p_1^2 + t_{12} t_{23} (M_1 - m) p_2^2 + t_{13} t_{23} m p_3^2}{2(t_{12} M_1 M_2 + t_{13} M_1 m + t_{23} M_2 m)}\right). \tag{12}
\end{aligned}$$

We can go to the CM frame by setting $\mathbf{p}_3 = 0$ and $|\mathbf{p}_1| = |\mathbf{p}_2| = p$. In the case $t_{12} > 0$, the 3-point function with the momentum delta function factored out reduces to

$$\begin{aligned}
& C'_{12,3}(t_{13})^{(D-\Delta_{13,2})/2} \theta(t_{13})(t_{23})^{(D-\Delta_{23,1})/2} \theta(t_{23}) |t_{12}|^{-\Delta_{12,3}/2} \int_0^\infty dm m^{\Delta_{12,3}/2-1} e^{-m\epsilon} \\
&\quad \times \int_{-\infty}^{+\infty} du (u + i\epsilon)^{-\Delta_{13,2}/2} e^{-i(M_1-m)u} \int_{-\infty}^{+\infty} dv (v + i\epsilon)^{-\Delta_{23,1}/2} e^{-i(M_2+m)v} \\
&\quad \times \left(\frac{t_{12} M_1 M_2}{t_{12} M_1 M_2 + t_{13} M_1 m + t_{23} M_2 m}\right)^{D/2} \exp\left(-i \frac{t_{12}(t_{23} M_1 + t_{13} M_2 + t_{12} m)}{2(t_{12} M_1 M_2 + t_{13} M_1 m + t_{23} M_2 m)} p^2\right), \tag{13}
\end{aligned}$$

where $C'_{12,3}$ is a constant. The integrals over u and v can be evaluated analytically by closing the integration contour in the lower half-plane,

$$\int_{-\infty}^{+\infty} du (u + i\epsilon)^{-\Delta/2} e^{-iMu} = e^{-i\pi\Delta/4} \frac{2\pi}{\Gamma(\Delta/2)} M^{\Delta/2-1} \theta(M). \tag{14}$$

After these integrals have been evaluated, the limit $\epsilon \rightarrow 0$ can be taken in the remainder. The choice $t_{12} > 0$ breaks the symmetry under interchange of the subscripts 1 and 2. Given this choice, it is convenient to change to a dimensionless integration variable $x = m/M_1$. Our final result for the spatial Fourier transform of the 3-point function in the CM frame with $t_{12} > 0$ is

$$\begin{aligned}
& C''_{12,3}(t_{13})^{(D-\Delta_{13,2})/2} \theta(t_{13})(t_{23})^{(D-\Delta_{23,1})/2} \theta(t_{23}) |t_{12}|^{-\Delta_{12,3}/2} \int_0^1 dx x^{\Delta_{12,3}/2-1} (1-x)^{\Delta_{13,2}/2-1} [1 + (M_1/M_2)x]^{\Delta_{23,1}/2-1} \\
&\quad \times \left(\frac{t_{12}}{t_{12} + (M_1/M_2)xt_{13} + xt_{23}}\right)^{D/2} \exp\left(-i \frac{t_{12}[xt_{12} + (M_2/M_1)t_{13} + t_{23}]}{2M_2[t_{12} + (M_1/M_2)xt_{13} + xt_{23}]} p^2\right), \tag{15}
\end{aligned}$$

where $C''_{12,3}$ is a constant.

D. Fourier transform in time

The Fourier transforms in the three times can be expressed as the product of the energy-conserving delta function $\delta(E_1 + E_2 - E_3)$, a Fourier transform in t_{13} with energy E_1 , and a Fourier transform in t_{23} with energy E_2 . We first isolate the contribution from the Fourier transform in t_{13} from the region $t_{13} \gg t_{23}$ and then evaluate the Fourier transform in t_{23} .

In the limit $t_{13} \gg t_{23}$, the exponential in Eq. (15), reduces to

$$\exp\left(-i \frac{t_{12}[xt_{12} + (M_2/M_1)t_{13} + t_{23}]}{2M_2[t_{12} + (M_1/M_2)xt_{13} + xt_{23}]} p^2\right) \longrightarrow \exp\left(-i \frac{p^2}{2M_1} t_{13}\right) \exp\left(-i \frac{[1 - 2x - (M_2/M_1)x] p^2}{2M_2[1 + (M_1/M_2)x]} t_{23}\right), \tag{16}$$

where the identity $t_{12} = t_{13} - t_{23}$ has been used. The contribution to the Fourier transform in t_{13} from the region $t_{13} \gg t_{23}$ can be reduced to the integral

$$\int_0^\infty dt_{13} (it_{13})^{(D-\Delta_{13,2}-\Delta_{12,3})/2} \exp\left(iE_1 t_{13} - i \frac{p^2}{2M_1} t_{13}\right) = -i\Gamma(D/2 + 1 - \Delta_1) \left(\frac{p^2}{2M_1} - E_1\right)^{\Delta_1 - D/2 - 1}. \tag{17}$$

This integral is the propagator for ϕ_1 multiplied by a constant. The subsequent Fourier transform in t_{23} can be reduced to the integral

$$\begin{aligned} & \int_0^\infty dt_{23} (it_{23})^{(D-\Delta_{23,1})/2} \exp\left(iE_2 t_{23} - i \frac{[1-2x - (M_2/M_1)x]p^2}{2M_2[1 + (M_1/M_2)x]} t_{23}\right) \\ &= -i\Gamma([D - \Delta_{23,1}]/2 + 1) \left(\frac{[1-2x - (M_2/M_1)x]p^2}{2M_2[1 + (M_1/M_2)x]} - E_2\right)^{(\Delta_{23,1}-D)/2-1}. \end{aligned} \quad (18)$$

We now specialize to the case of $\phi_1(x)$ being the operator that annihilates a single particle. Its scaling dimension is $\Delta_1 = D/2$, so the integral in Eq. (17) has a simple pole at $E_1 = p^2/(2M_1)$. The residue of the pole in the Fourier-transformed three-point function is

$$\begin{aligned} G_{\text{pole}}(E_2, p) &= C_{12,3}''' \int_0^1 dx x^{\Delta_{12,3}/2-1} (1-x)^{\Delta_{13,2}/2-1} [1 + (M_1/M_2)x]^{\Delta_{23,1}/2-1-D/2} \\ &\times \left(\frac{p^2}{2M_2} - E_2 - \frac{(M_3/M_2)x}{1 + (M_1/M_2)x} \frac{p^2}{2M_{12}}\right)^{(\Delta_{23,1}-D)/2-1}, \end{aligned} \quad (19)$$

where $M_{12} = M_1 M_2 / M_3$ is a reduced mass and $C_{12,3}'''$ is a constant. The integrand has been expressed as a function of the energy $E_2 - p^2/(2M_2)$ of the unparticle relative to its threshold and the total energy $p^2/(2M_{12})$ of the unparticle at its threshold and the particle.

In the limit $E_2 \rightarrow p^2/(2M_2)$ with p^2 fixed, the integral over x in Eq. (19) has a divergent term that comes from the region near the lower endpoint. The divergent factor is the propagator of the unparticle. The limiting behavior of the 3-point function in Eq. (19) as $E_2 \rightarrow p^2/(2M_2)$ is

$$G_{\text{pole}}(E_2, p) \rightarrow C_{12,3}'''' D_2(E_2, p) \left(\frac{p^2}{2M_{12}}\right)^{-\Delta_{12,3}/2}, \quad (20)$$

where $C_{12,3}''''$ is a constant. This is our result for the scaling behavior of the Fourier-transformed 3-point function at large momentum p .

The exponent $-\Delta_{12,3}/2$ in Eq. (20) can also be deduced from the analytic result for an integral whose integrand has the same dependence on x near the lower endpoint as the integrand in Eq. (19),

$$\begin{aligned} & \int_0^1 dx x^{\Delta_{12,3}/2-1} (1-x)^{\Delta_{13,2}/2-1} \left(\frac{p^2}{2M_2} - E_2 - x(M_3/M_2) \frac{p^2}{2M_{12}}\right)^{(\Delta_{23,1}-D)/2-1} \\ &= B\left(\frac{\Delta_{12,3}}{2}, \frac{\Delta_{13,2}}{2}\right) \left(\frac{p^2}{2M_2} - E_2\right)^{(\Delta_{23,1}-D)/2-1} {}_2F_1\left(\frac{\Delta_{12,3}}{2}, \frac{D+2-\Delta_{23,1}}{2}; \Delta_1; \frac{(M_3/M_2)(p^2/2M_{12})}{p^2/(2M_2) - E_2}\right), \end{aligned} \quad (21)$$

where $B(x, y)$ is the beta function and ${}_2F_1(a, b; c; z)$ is the ordinary hypergeometric function (cf. Ref. [21]). Using the transformation formula that changes the argument of the hypergeometric function from z to $1/z$, we find that its leading divergence as $z \rightarrow \infty$ has the factor $z^{-\Delta_{12,3}/2}$ provided $D > 2$.

III. POINT PRODUCTION RATES

We are now in the position to determine the energy dependence of the production rate of an unparticle recoiling against a particle with large relative momentum from the creation of an unparticle at short distances. We then determine the exponent of the energy in the production rate of a loosely bound 2-particle state recoiling against a

particle with large relative momentum. For definiteness, we focus on the case $D = 3$.

A. Unparticle recoiling against a particle

We first consider the production rate in the NRCFT of a particle with mass M_1 plus the unparticle with mass M_2 and scaling dimension Δ_2 from the creation at short distances of the unparticle with mass $M_3 = M_2 + M_1$ and scaling dimension Δ_3 . The inclusive production rate is proportional to the imaginary part of the Green function $\langle \phi_3(x_1) \phi_3^\dagger(x_2) \rangle$. The contribution to the production rate from intermediate states consisting of a particle and an unparticle can be obtained from the Fourier transform of the 3-point function $\langle \phi_1(x_1) \phi_2(x_2) \phi_3^\dagger(x_3) \rangle$ in the CM frame, which we denote

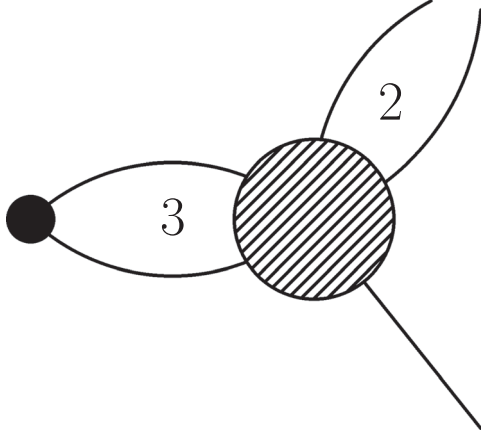


FIG. 5. Amplitude for the creation of unparticle 3 at a point and its evolution to unparticle 2 and a single particle with large relative momentum. The particle is represented by a single line.

as $G(E_1, E_2, p)$. The Green function $G(E_1, E_2, p)$ with the particle propagator $D_1(E_1, p)$ amputated and evaluated on shell at $E_1 = p^2/(2M)$ is $G_{\text{pole}}(E_2, p)$ in Eq. (19). That amplitude can be represented by the diagram in Fig. 5. By energy conservation, the total energy is $E_3 = E_1 + E_2$. Using the optical theorem, the differential rate dR as a function of the total energy E_3 can be obtained from $G_{\text{pole}}(E_2, p)$ in several steps:

- (i) complete the amputation of the final-state propagators by dividing $G_{\text{pole}}(E_2, p)$ by the unparticle propagator $D_2(E_2, p)$,
- (ii) multiply the amputated amplitude $G_{\text{amp}}(E_2, p) = G_{\text{pole}}(E_2, p)/D_2(E_2, p)$ by its complex conjugate,
- (iii) multiply $|G_{\text{amp}}(E_2, p)|^2$ by the discontinuities in the particle propagator $D_1(E_1, p)$ and in the unparticle propagator $D_2(E_2, p)$, which are given in Eqs. (5) and (6),
- (iv) integrate over the energy E_1 of the particle and its momentum \mathbf{p} in the CM frame with the measure $dE_1 d^3 p / (2\pi)^4$.

The resulting expression for the differential production rate in the CM frame as a function of E_3 is

$$dR = C \int \frac{dE_1}{2\pi} \frac{d^3 p}{(2\pi)^3} |G_{\text{amp}}(E_3 - E_1, p)|^2 2\pi \delta\left(E_1 - \frac{p^2}{2M_1}\right) \times \left(E_3 - E_1 - \frac{p^2}{2M_2}\right)^{\Delta_2 - 5/2} \theta\left(E_3 - E_1 - \frac{p^2}{2M_2}\right), \quad (22)$$

where C is a constant. The integral over E_1 can be evaluated using the delta function, which sets $E_1 = p^2/(2M_1)$. The discontinuity in $D_2(E_2, p)$ provides the threshold $E_3 > p^2/(2M_{12})$, where $M_{12} = M_1 M_2 / M_3$ is a reduced mass. The differential rate for E_3 above the threshold reduces to

$$dR = C \left(E_3 - \frac{p^2}{2M_{12}}\right)^{\Delta_2 - 5/2} \times |G_{\text{amp}}(E_3 - p^2/(2M_1), p)|^2 \frac{d^3 p}{(2\pi)^3}. \quad (23)$$

We can use Eq. (20) to deduce the rate for energy E_3 close to the threshold $p^2/(2M_{12})$ for fixed p . The limiting behavior as $E_2 \rightarrow p^2/(2M_2)$ of the amputated 3-point function is

$$G_{\text{amp}}(E_2, p) \rightarrow C_{12,3}'''' \left(\frac{p^2}{2M_{12}}\right)^{-\Delta_{12,3}/2}. \quad (24)$$

The limiting behavior of the differential rate as $E_3 \rightarrow p^2/(2M_{12})$ is therefore

$$dR \rightarrow C' \left(E_3 - \frac{p^2}{2M_{12}}\right)^{\Delta_2 - 5/2} \left(\frac{p^2}{2M_{12}}\right)^{\Delta_3 - \Delta_2 - 3/2} \frac{d^3 p}{(2\pi)^3}, \quad (25)$$

where $C' = C_{12,3}'''' C$ and we have used $\Delta_1 = 3/2$.

The above results for the point-production rate in Eq. (25) can be applied to multineutron systems. In this case, Δ_3 and Δ_2 are the scaling dimensions of $(N+1)$ -neutron and N -neutron operators, respectively. The contribution to the point production rate of the $(N+1)$ -neutron unparticle from its decay into an N -neutron unparticle recoiling against a single neutron is given by Eq. (23). In the region near the threshold for the N -neutron unparticle, that production rate reduces at large relative momentum to Eq. (25). The lowest scaling dimensions for 3, 4, and 5 neutrons are 4.27, 5.07, 7.6, respectively. (See [10] for further discussion and references.)

B. Bound state recoiling against a particle

Next we consider the case where a bound state arises from a deformation of a nonrelativistic conformal field theory that produces a large positive scattering length a in the channel associated with the unparticle with mass M_2 and scaling dimension $\Delta_2 = 2$. The bound state has constituents with masses M_1 and $M_2 - M_1$. Its binding energy is $|\epsilon_X| = 1/(2\mu a^2)$, where $\mu = M_1(M_2 - M_1)/M_2$ is the reduced mass of its constituents. The field $\phi_2^\dagger(x)$ creates a particle of mass M_1 and a particle of mass $M_2 - M_1$. The propagator for the field $\phi_2(x)$ is

$$D_2(E, p) = -iC_2' \left[\left(\frac{p^2}{2M_2} - E\right)^{1/2} - \frac{1}{\sqrt{2\mu a^2}} \right]^{-1}. \quad (26)$$

This propagator has a pole at the energy

$$E_{\text{pole}} = -\frac{1}{2\mu a^2} + \frac{p^2}{2M_2}. \quad (27)$$

The pole is associated with the bound state, which we will refer to as X . The discontinuity of the propagator is

$$\begin{aligned} & D_2(E + i\epsilon, p) - D_2(E - i\epsilon, p) \\ &= 2C'_2 \left[\frac{\sqrt{E - p^2/(2M_2)}}{E - p^2/(2M_2) + |\epsilon_X|} \theta\left(E - \frac{p^2}{2M_n}\right) \right. \\ & \quad \left. + 2\pi\sqrt{|\epsilon_X|} \delta\left(E + |\epsilon_X| - \frac{p^2}{2M_2}\right) \right]. \end{aligned} \quad (28)$$

The differential rate dR for the production of either three particles or a single particle plus X can be obtained from the differential rate in Eq. (22) by taking into account the dependence of $G_{\text{amp}}(E_3 - E_1, p)$ on a and replacing the discontinuity of the propagator $D_2(E_3 - E_1, p)$ by the discontinuity given in Eq. (28). The amplitude for producing the bound state X plus a single particle can be represented by the diagram in Fig. 6. The integrated rate R_X for producing a single particle plus X can be obtained by using the delta function in Eq. (28) to evaluate the integral over \mathbf{p} in Eq. (23),

$$\begin{aligned} R_X &= C_X \sqrt{|\epsilon_X|} (E_3 + |\epsilon_X|)^{1/2} \\ & \quad \times \left| G_{\text{amp}}\left(\frac{M_1 E_3 - M_2 |\epsilon_X|}{M_3}, [2M_{12}(E_3 + |\epsilon_X|)]^{1/2}\right) \right|^2, \end{aligned} \quad (29)$$

where $C_X = CC'_2(2M_{12})^{3/2}/\pi$. The amputated 3-point function depends on a explicitly through ϵ_X in its two arguments and also implicitly through the interactions between the particles. In the limit $E_3 \gg |\epsilon_X|$, its dependence on E_3 is given in Eq. (20). The dependence of R_X on E_3 in that limit therefore has the power-law behavior

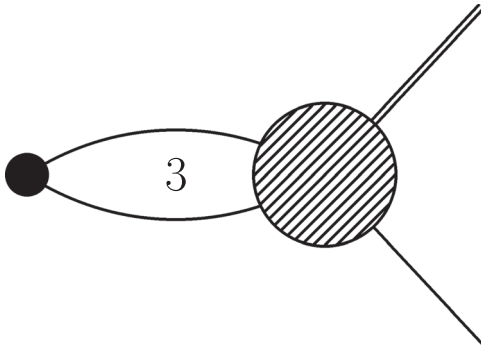


FIG. 6. Amplitude for the creation of unparticle 3 at a point and its evolution to a loosely bound state of two particles and a single particle with large relative momentum. The bound state is represented by a double line.

$$R_X \rightarrow C'_X \sqrt{|\epsilon_X|} E_3^{-\Delta_{12,3}+1/2}, \quad (30)$$

where C'_X is a constant. The exponent is $\Delta_3 - \Delta_2 - \Delta_1 + \frac{1}{2} = \Delta_3 - 3$.

This case can be realized with neutral D and D^* mesons and the $X(3872)$ [13]. The $X(3872)$ is a resonance extremely close to the threshold in the $J^{PC} = 1^{++}$ channel of $D^{*0}\bar{D}^0$ and $D^0\bar{D}^{*0}$. The most precise measurements of the mass by the LHCb Collaboration give an energy relative to the $D^{*0}\bar{D}^0$ threshold of $\epsilon_X = -0.07 \pm 0.12$ MeV [22,23], which implies $|\epsilon_X| < 0.22$ MeV at the 90% confidence level. This tiny binding energy corresponds to a large positive scattering length $a = 1/\sqrt{2\mu|\epsilon_X|}$, where μ is the $D^{*0}\bar{D}^0$ reduced mass.

The production rate dR/dE of an X and a neutral D or D^* meson near the threshold is determined by the energy scale $\epsilon_{DX} = 1/(2\mu_{DX}a_{DX}^2)$, where μ_{DX} is the reduced mass of the XD (or XD^*) system and a_{DX} is the corresponding S -wave scattering length. To leading order in the contact effective field theory for the neutral D and D^* mesons, the scattering lengths for D^0X and $D^{*0}X$ are universal and equal to a multiplied by a large negative coefficient: $a_{D^0X} = -9.7a$, $a_{D^{*0}X} = -16.6a$ [24]. Thus they show an additional enhancement beyond the already large $D^{*0}\bar{D}^0$ scattering length a . Inserting explicit values leads to the tiny energy scales $\epsilon_{D^0X} = 0.82$ keV or $\epsilon_{D^{*0}X} = 0.26$ keV.

As shown in Fig. 7, dR/dE increases from zero at the threshold to a peak near $\epsilon_{DX}/|\epsilon_X| \approx 0.01$ for D^0X and 0.004 for $D^{*0}X$, respectively. Then it decreases to a local minimum at an energy of order $|\epsilon_X|$. In this region, the interior structure of the X is not resolved and the scaling exponent $-1/2$ for two structureless particles in the final state appears [8]. Beyond the minimum, there is a scaling region where dR/dE increases with a power-law determined by the three-body scaling dimensions $\Delta_3 = 3.10119$

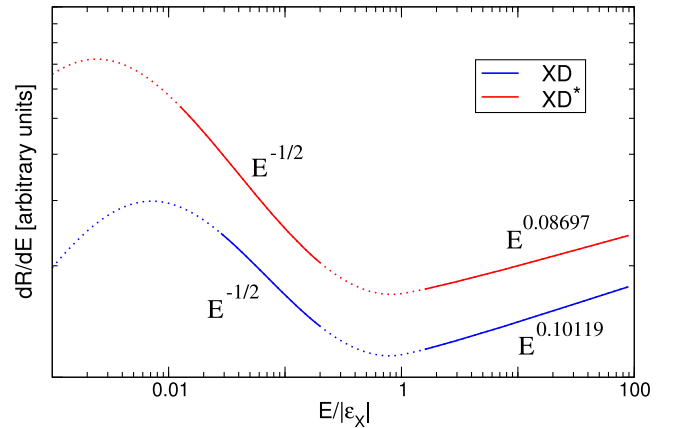


FIG. 7. Production rates dR/dE for D^0X (solid curve) and $D^{*0}X$ (dashed curve) from the creation of neutral charm mesons at short distances as functions of the invariant energy E . The dotted lines show the transition between different scaling regions.

for D^0X and $\Delta_3 = 3.08697$ for $D^{*0}X$. The power-law behavior of the amplitudes Γ for D^0X and $D^{*0}X$ is predicted as $E^{0.10119}$ and $E^{0.08697}$, respectively [13]. It has been verified by explicit calculations of the point production rate in a contact effective field theory for the neutral D and D^* mesons. There is a crossover to a more rapidly-increasing production rate at even higher energies when nonuniversal effects kick in, which is not shown in Fig. 7.

IV. CONCLUSION

Nonrelativistic unparticles arise naturally in any system that can be described by a nonrelativistic field theory close to a conformally invariant limit. Systems of neutrons with small invariant energy created by point reactions are examples of nonrelativistic unparticles in nuclear physics [8]. Systems of neutral charm mesons with small invariant energy created by point reactions are examples of nonrelativistic unparticles in particle physics [13]. The concept of nonrelativistic unparticles is useful, because it allows scaling regions to be identified in which reaction rates have power-law behavior characterized by nontrivial exponents. It would be interesting to find other physical realizations of nonrelativistic unparticles in nature. It would also be interesting to exploit the remarkable control of interactions that is possible with ultracold atoms to create new systems with unparticles.

We have used the analytic results for the three-point function for primary operators in a nonrelativistic

conformal field theory in Refs. [18–20] to derive the contribution to the point production rate of an unparticle from its decay into another unparticle recoiling against a particle. We also used it to derive a scaling law for the decay into a loosely bound 2-particle state recoiling against a particle with large momentum. If analytic results for the 4-point function of primary operators in a nonrelativistic conformal field theory were available, they could be applied to the elastic scattering of unparticles or the elastic scattering of an unparticle with a particle. They could also be used to derive scaling laws for the elastic scattering of a loosely bound 2-particle state and a particle at large momentum transfer. It would be interesting to compare the analytic exponents with numerical results for the elastic scattering of D^0 and D^{*0} with $X(3872)$ [13].

ACKNOWLEDGMENTS

H.-W.H. acknowledges the hospitality of KITP, Santa Barbara where part of this work was carried out. The research of E.B. was supported in part by the U.S. Department of Energy under Grant No. DE-SC0011726. H.-W.H. was supported in part by the National Science Foundation under Grant No. NSF PHY-1748958, by the Deutsche Forschungsgemeinschaft (DFG, German Research Foundation), Project ID 279384907—SFB 1245 and by the German Federal Ministry of Education and Research (BMBF) (Grant No. 05P21RDFNB).

-
- [1] H. Georgi, Unparticle Physics, *Phys. Rev. Lett.* **98**, 221601 (2007).
 - [2] K. Cheung, W. Y. Keung, and T. C. Yuan, Collider Signals of Unparticle Physics, *Phys. Rev. Lett.* **99**, 051803 (2007).
 - [3] H. Georgi, Another odd thing about unparticle physics, *Phys. Lett. B* **650**, 275 (2007).
 - [4] K. Cheung, W. Y. Keung, and T. C. Yuan, Collider phenomenology of unparticle physics, *Phys. Rev. D* **76**, 055003 (2007).
 - [5] V. Khachatryan *et al.* (CMS Collaboration), Search for dark matter, extra dimensions, and unparticles in monojet events in proton–proton collisions at $\sqrt{s} = 8$ TeV, *Eur. Phys. J. C* **75**, 235 (2015).
 - [6] V. Khachatryan *et al.* (CMS Collaboration), Search for dark matter and unparticles produced in association with a Z boson in proton-proton collisions at $\sqrt{s} = 8$ TeV, *Phys. Rev. D* **93**, 052011 (2016); **97**, 099903(E) (2018).
 - [7] A. M. Sirunyan *et al.* (CMS Collaboration), Search for dark matter and unparticles in events with a Z boson and missing transverse momentum in proton-proton collisions at $\sqrt{s} = 13$ TeV, *J. High Energy Phys.* 03 (2017) 061; 09 (2017) 106(E).
 - [8] H. W. Hammer and D. T. Son, Unnuclear physics, *Proc. Natl. Acad. Sci. U.S.A.* **118**, e2108716118 (2021).
 - [9] G. K. Karananas and A. Monin, More on the operator-state map in nonrelativistic CFTs, *Phys. Rev. D* **105**, 065008 (2022).
 - [10] Y. Nishida and D. T. Son, Nonrelativistic conformal field theories, *Phys. Rev. D* **76**, 086004 (2007).
 - [11] M. Duer *et al.*, Observation of a correlated free four-neutron system, *Nature (London)* **606**, 678 (2022).
 - [12] R. Lazauskas, E. Hiyama, and J. Carbonell, Low energy structures in nuclear reactions with 4n in the final state, [arXiv:2207.07575](https://arxiv.org/abs/2207.07575).
 - [13] E. Braaten and H. W. Hammer, Interpretation of Neutral Charm Mesons near Threshold as Unparticles, *Phys. Rev. Lett.* **128**, 032002 (2022).
 - [14] S. K. Choi *et al.* (Belle Collaboration), Observation of a Narrow Charmonium-Like State in Exclusive $B^\pm \rightarrow K^\pm \pi^+ \pi^- J/\psi$ Decays, *Phys. Rev. Lett.* **91**, 262001 (2003).

- [15] E. Braaten and M. Kusunoki, Low-energy universality and the new charmonium resonance at 3870-MeV, *Phys. Rev. D* **69**, 074005 (2004).
- [16] E. Braaten and H. W. Hammer, Universality in few-body systems with large scattering length, *Phys. Rep.* **428**, 259 (2006).
- [17] M. Henkel, Schrodinger invariance in strongly anisotropic critical systems, *J. Stat. Phys.* **75**, 1023 (1994).
- [18] M. Henkel and J. Unterberger, Schrodinger invariance and space-time symmetries, *Nucl. Phys.* **B660**, 407 (2003).
- [19] C. A. Fuertes and S. Moroz, Correlation functions in the non-relativistic AdS/CFT correspondence, *Phys. Rev. D* **79**, 106004 (2009).
- [20] A. Volovich and C. Wen, Correlation functions in non-relativistic holography, *J. High Energy Phys.* **05** (2009) 087.
- [21] I. S. Gradshteyn and I. M. Ryzhik, *Table of Integrals, Series, and Products* (Academic Press, New York, 1965).
- [22] R. Aaij *et al.* (LHCb Collaboration), Study of the line-shape of the $\chi_{c1}(3872)$ state, *Phys. Rev. D* **102**, 092005 (2020).
- [23] R. Aaij *et al.* (LHCb Collaboration), Study of the $\psi_2(3823)$ and $\chi_{c1}(3872)$ states in $B^+ \rightarrow (J/\psi\pi^+\pi^-)K^+$ decays, *J. High Energy Phys.* **08** (2020) 123.
- [24] D. L. Canham, H.-W. Hammer, and R. P. Springer, On the scattering of D and D^* mesons off the $X(3872)$, *Phys. Rev. D* **80**, 014009 (2009).